Environmental Pollution 337 (2023) 122549

Contents lists available at ScienceDirect

Environmental Pollution

journal homepage: www.elsevier.com/locate/envpol

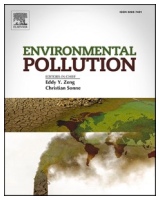

Does functionalised nanoplastics modulate the cellular and physiological responses of aquatic fungi to metals?☆

Juliana Barros [a], Santosh Kumar [b,c], Sahadevan Seena [a,*]

[a] Marine and Environmental Sciences Centre (MARE)/Rede de Investigação Aquática (ARNET), Department of Life Sciences, University of Coimbra, Calçada Martim de Freitas, 3000-456 Coimbra, Portugal
[b] Division of Chemical Engineering, Konkuk University, Seoul 05029, South Korea
[c] Department of Chemistry, School of Basic & Applied Sciences, Harcourt Butler Technical University, Kanpur 208002 Uttar Pradesh, India

ARTICLE INFO

Keywords:
Aquatic hyphomycetes
Polystyrene
Freshwaters
Plastic pollution
Copper

ABSTRACT

Co-contamination of freshwaters by nanoplastics (NPs; ≤ 1 μm) and metals is an emerging concern. Aquatic hyphomycetes play a crucial role as primary decomposers in these ecosystems. However, concurrent impacts of NPs and metals on the cellular and physiological activities of these fungi remain poorly understood. Here, the effects of environmentally realistic concentrations of two types of polystyrene (PS) NPs (bare and –COOH; up to 25 μg L^{-1}) and copper (Cu; up to 50 μg L^{-1}) individually and all possible combinations (NPs types and Cu) on *Articulospora tetracladia*, a prevalent aquatic hyphomycete, were investigated. Endpoints measured were intracellular reactive oxygen species accumulation, plasma membrane disruption and fungal growth. The results suggest that functionalised (–COOH) NPs enhance Cu adsorption, as revealed by spectroscopic analyses. Notably, NPs, Cu and their co-exposure to *A. tetracladia* can lead to ROS accumulation and plasma membrane disruption. In most cases, exposure to treatments containing –COOH NPs with Cu showed greater cellular response and suppressed fungal growth. By contrast, exposure to Cu individually showed stimulatory effects on fungal growth. Overall, this study provides novel insight that functionalisation of NPs facilitates metal adsorption, thus modulating the impacts of metals on aquatic fungi.

1. Introduction

Over the past few decades, the levels of plastic pollution have risen to an unparalleled extent, making it one of the most pressing environmental issues of the 21st century (Thompson et al., 2009). According to recent estimates (Boucher and Friot, 2017; Jambeck et al., 2015), the current annual input of plastics into the ocean via river systems is approximately 9.5 million metric tons. Moreover, significant progress in nanotechnology has facilitated the widespread production and utilisation of nanoplastics (NPs, ≤ 1 μm) (Gigault et al., 2021, 2018; Hartmann et al., 2019). NPs find wide-ranging applications in various sectors, including electronics, energy, healthcare, and agriculture (Kumar et al., 2021; Prasad et al., 2017). Besides, surface modification of plastics enables the introduction of desired functionalities, such as improved adhesion, wettability or biocompatibility, broadening their applications. For instance, carboxyl (–COOH) functionalised NPs are utilised in targeted drug delivery and environmental remediation purposes (Aitken et al., 2006; Nath et al., 2020; Salata, 2004). Despite the growing utilisation of NPs, there is currently a dearth of comprehensive data regarding their market size and overall extent. However, owing to their distinctive attributes such as robustness, longevity, and thermal stability, there is an anticipated surge in the demand and production of NPs in the forthcoming years. For example, polymeric nanoparticles market was valued at approximately US$ 551.9 million in 2020 and is projected to grow at a compound annual growth rate (CAGR) of 10.6% by 2030 (www.alliedmarketresearch.com). Nevertheless, accurate identification and quantification of NPs released into the environment are currently impeded by the lack of appropriate analytical tools. Advancements in these research areas are crucial for comprehending the properties, behaviour, and potential risks associated with NPs in aquatic ecosystems, which serve as their ultimate repositories (Kumar et al., 2021). Similar to conventional plastics, NPs such as polystyrene (PS) NPs, frequently used in electronics, medicine and cosmetics, can persist for hundreds of years without decomposing,

☆ This paper has been recommended for acceptance by Eddy Y. Zeng.

* Corresponding author.
E-mail addresses: seena.sahadevan@gmail.com, seena.sahadevan@uc.pt (S. Seena).

https://doi.org/10.1016/j.envpol.2023.122549
Received 18 July 2023; Received in revised form 2 September 2023; Accepted 12 September 2023
Available online 18 September 2023

thereby presenting potential hazards to the environment and wildlife (Gottschalk and Nowack, 2011; Mattsson et al., 2018; Mueller and Nowack, 2008; Nowack et al., 2012). In addition to their intentional manufacture, NPs are also formed by fragmentation of bulk plastics due to weathering processes such as biodegradation, hydrolysis and light (Gigault et al., 2018; Tallec et al., 2019; Y. Zhang et al., 2022). These processes play a significant role in modifying the physicochemical characteristics of NPs. For instance, weathering-induced surface oxidation can lead to alterations in the chemical and physical properties of NPs, thereby affecting their aggregation behaviour (Li et al., 2020; Tallec et al., 2019), migration patterns (Dong et al., 2019), hydrophobicity (Li et al., 2020), and adsorption capacity (Liu et al., 2018). Surface oxidation involves the introduction of oxygen-containing chemical groups onto the NP surface, such as −COOH groups (Nolte et al., 2017; Tallec et al., 2019; Wang et al., 2021) resulting in a negatively charged NP surface. The presence of newly formed –COOH groups can significantly influence the interactions of NPs with other molecules, with implications on their bioavailability and toxicity (Della Torre et al., 2014; Zhang et al., 2019).

Once discharged into the freshwaters, NPs containing –COOH groups (up to 0.1 g L^{-1}) have demonstrated greater toxicity towards periphyton biofilms compared to bare NPs (up to 0.1 g L^{-1}), leading to increased oxidative stress and cell membrane damage (Miao et al., 2019). Furthermore, –COOH groups enhance the adsorption capacity of NPs to organic pollutants and metals (González-Fernández et al., 2021; Liu et al., 2018; Naqash et al., 2020), emphasising their role as a potential source of these pollutants (Munier and Bendell, 2018). For example, –COOH NPs (up to 0.1 g L^{-1}) contributed to the toxicity enhancement of arsenic (up to 7.5 g L^{-1}) and methylmercury (up to 21.5 g L^{-1}) in fish brain-derived cells (González-Fernández et al., 2021).

Freshwaters are particularly vulnerable to emerging contaminants, as they serve as the primary interface between terrestrial and aquatic compartments, receiving inputs from both land and water sources. Therefore, they are often more susceptible to adverse effects of emerging contaminants when compared to other environmental compartments. Mining activities contribute to the widespread occurrence of metals in freshwater systems, leading to the co-existence of metals with emerging contaminants such as NPs. Among these metals, copper (Cu) stands out as a prominent pollutant, with concentrations reaching levels as high as 10 mg L^{-1} (Sridhar et al., 2000) particularly in European streams (Krauss et al., 2011). Although Cu is an essential micronutrient, its elevated concentrations can interfere with numerous biochemical processes by inhibiting enzymes and inducing oxidative stress through the generation of reactive oxygen species (ROS) (Avery, 2001; Braha et al., 2007). When ROS levels surpass the cellular detoxification capacity, they can induce damage by compromising the cellular redox potential, leading to lipid peroxidation and subsequent impairment of the plasma membrane (Avery, 2001; Petersen and Nelson, 2010) as well as mitochondrial membrane depolarisation (Pradhan et al., 2015) and growth (Pradhan et al., 2014).

Aquatic fungi, particularly aquatic hyphomycetes, hold significant importance in freshwater ecosystems as they contribute to the decomposition of organic matter. This process is vital for sustaining the functioning and overall health of the ecosystem (Gessner et al., 1999; Gessner and Chauvet, 2002; Graça and Canhoto, 2006). The enzymatic activities of aquatic hyphomycetes are responsible for the breakdown of structural components of organic matter, resulting in the release of essential nutrients. These nutrients are fundamental for the growth and survival of various other organisms within the ecosystem. Aquatic hyphomycetes improve the palatability and nutritional quality of organic matter for invertebrates (Cummins, 1973; Cummins and Klug, 1979; Graça, 2001), promoting energy transfer throughout the freshwater food web (Graça and Canhoto, 2006). These fungi are known to be particularly sensitive to anthropogenic stressors (Ferreira et al., 2016; Solé et al., 2008), which lead to detrimental effects on their survival, growth and activity (Azevedo and Cássio, 2010; Ferreira et al., 2016). Notably, the exposure to PS NPs (1×10^{-6} and 1×10^{-4} g L^{-1}) impacted the growth and enzyme activity of aquatic hyphomycete communities by interfering with the nutrient uptake mechanisms (Du et al., 2022). Moreover, PS NPs have been found to diminish the decomposition capacity of these fungi, with significant implications for freshwater ecosystems (Du et al., 2022). Similarly, metals such as Cu (up to 0.63 g L^{-1}) can exert harmful effects on aquatic hyphomycetes leading to decreased leaf decomposition rates, impaired fungal reproduction and reduced biomass production (Duarte et al., 2008). In addition, Cu can exert higher toxicity than zinc on multiple species of aquatic hyphomycetes (Duarte et al., 2008). Moreover, the exposure to nano copper oxide (up to 0.2 g L^{-1}) induced oxidative stress in aquatic hyphomycetes as demonstrated by the concentration-dependent intracellular accumulation of ROS, plasma membrane damage, and DNA strand breaks (Pradhan et al., 2015).

In recent years, there has been growing interest in understanding the combined effects of pollutants on freshwater organisms due to the frequent occurrence of multiple pollutants in freshwater environments. NPs and metals are among the prominent contaminants found in such settings, and their co-existence is an unavoidable reality. Co-existing environmental contaminants can interact, altering their bioavailability and toxicity to freshwater organisms. The goal of this study was to provide insights into the concomitant effects of NPs and Cu on the vital cellular processes and overall growth of a common wide-spread aquatic hyphomycetes *Articulospora tetracladia* (ARTE; Seena et al., 2012, 2018; 2012). The cellular and physiological responses of ARTE to two different types of NPs (bare and –COOH), as well as Cu, both individually and in various combinations of NPs types with Cu, were investigated. The study focused on environmentally realistic concentrations of these NPs (0.25, 2.5, and 25 μg L^{-1}) and their combinations with Cu (25 and 50 μg L^{-1}). ARTE is highly susceptible to the presence of pollutants, which can adversely affect its ability to decompose organic matter. Notably, previous studies have shown that nano copper oxide (0.12 mg L^{-1}) and PS NPs (102.4 mg L^{-1}) reduced the leaf litter decomposition ability of ARTE (Seena et al., 2019; Seena and Kumar, 2019). Here, it was hypothesised that increasing concentrations of PS NPs and Cu would have detrimental effects on cellular activities and fungal growth (Pradhan et al., 2015). Besides, co-exposure of PS NPs types with Cu would modulate the adverse effects on fungi, given that NPs tend to influence metal toxicity by facilitating metal adsorption (Lee et al., 2019). This study was conducted in stream microcosms; the measured parameters were ROS and plasma membrane disruption to unravel the cellular activities and biomass production for fungal growth.

2. Materials and methods

2.1. Polystyrene nanoplastics

PS NPs are widely utilised as model NPs due to their ease of synthesis, enabling their production in various sizes and surface functionalisation. This feature of PS NPs contributes to their popularity as a versatile choice for mimicking different types of NPs (Kik et al., 2020; Loos et al., 2014). Bare and –COOH PS NPs with a nominal mean diameter, respectively of 70 and 60 nm, purchased from Spherotech Inc. (10,000 mg L^{-1} aqueous suspension) were used in this study. Suspension of bare NPs was provided in 1% deionised water, which included 0.02% sodium azide as a bacteriostatic preservative. On the other hand, the suspension of –COOH PS NPs was supplied in 1% deionised water (without sodium azide). To remove the sodium azide from the bare NPs suspension before the exposure experiment, dialysis was performed using a dialysis bag (molecular weight cut-off of 1000), against deionised water (Miao et al., 2019; Pikuda et al., 2019). In order to confirm that the concentration of the suspension remained consistent after the dialysis process, UV–visible spectra (Borowska and Jankowski, 2023; Minelli et al., 2019) was measured (Agilent 8453, USA). This allowed for a comparison of the suspensions before and after dialysis, ensuring that

there were no significant changes in the NPs concentration. In addition, inductively coupled plasma atomic emission (ICP-AES) spectrometry was evaluated (PerkinElmer Optima 4300DV, USA) to measure the sodium concentration after dialyses (Kumar et al., 2019). NPs aqueous suspensions were sonicated in an ultrasonic water bath (42 kHz, 100 W; Branson 2510, USA) for 10 min before use.

2.2. Microcosm experiment

The chosen nominal exposure concentrations of NPs were representative of the current low (0.25 μg L^{-1}) and high (2.5 μg L^{-1}) concentrations of microplastics found in aquatic systems (Jambeck et al., 2015; Lenz et al., 2016). Moreover, the highest concentration (25 μg L^{-1}) was selected to project a tenfold increase in the amount of plastic waste entering ecosystems by 2025 (Jambeck et al., 2015). The concentrations of Cu (25 and 50 μg L^{-1}) used in this study were chosen to mirror the average values observed in Iberian streams, which have a significant history of mining activities (Quainoo et al., 2016; Seena et al., 2020). For both PS NP types, a 25 μg L^{-1} of plastic suspension was accomplished by diluting the NPs (10,000 mg L^{-1}) in sterile 1% malt extract broth (GranuCult®, autoclaved, 120 °C, 20 min) containing 16 mg L^{-1} of streptomycin sulphate (Sigma-Aldrich) in order to avoid bacterial growth. The desired lower concentrations of 2.5 and 0.25 μg L^{-1} were achieved by performing successive dilutions of the NPs suspension at 25 g L^{-1} in the malt extract broth. A 50 mg L^{-1} Cu stock solution was prepared by adding 98.23 mg of copper (II) sulphate crystals ($CuSO_4{\cdot}5H_2O$; Sigma) and by stirring gently on a magnetic stirrer (10 min; Stuart Scientific, UK). Serial dilutions were then performed to obtain concentrations of 1 mg L^{-1}, followed by additional dilutions to achieve concentrations of 50 and 25 μg L^{-1} Cu. Further, the sterile Cu solution was obtained after passing through a filter (Ministart Syringe Filter; Sartorius) and added to the microcosms containing the respective concentrations of NPs prepared in 1% malt extract broth. The fungi, ARTE (MARE-UC-28-2019), isolated from a stream within a temperate deciduous forest (Margaraça Forest in Central Portugal) was used in this study. The effects were evaluated using 21 treatments with 15 replicates assigned to each treatment. The treatments included a control group (0 μg L^{-1} of NPs and Cu), Cu (25 and 50 μg L^{-1}), and NPs (0.25, 2.5 and 25 μg L^{-1}). Furthermore, mixtures containing all possible combinations of NPs and Cu (see Fig. S1) were included in the study. Endpoints measured were accumulation of intracellular ROS and plasma membrane integrity to evaluate the cellular responses as well as fungal biomass production to assess their growth (Fig. S1). Experimental procedure commenced by incubating the microcosms consisting of 25 mL of the respective exposure treatments. The incubation was carried out at a temperature of 18 °C for 24 h in the dark using an orbital shaker (120 rpm). Following this incubation period, fungal homogenates were inoculated into microcosms. For preparing fungal homogenates, an agar plug (12 mm diameter; 21 days old cultures) of ARTE grown on malt extract agar medium (1% w/v; agar and malt extract) at 18 °C was homogenised (Ultra Turrax IKA, Germany) in 1 mL sterile liquid medium (1% w/v; malt extract) and 0.25 mL of the homogenate was inoculated in a 100-mL Erlenmeyer flask containing 25 mL of the respective exposure treatments. Subsequently, microcosms were incubated on an orbital shaker (120 rpm) for 10 days under similar conditions. Among the replicates (n = 15), three sets were designated for the analysis of ROS accumulation and plasma membrane integrity of the fungal hyphae. Mycelial suspensions from these three sets were pooled before the assessments were conducted. Following the evaluation of ROS and plasma membrane integrity, suspensions were used for NPs characterisation. Remaining nine microcosms were dedicated to biomass quantification. An additional three replicates were maintained in the absence of fungal homogenate to eliminate any potential interference from the media during biomass quantification.

2.3. Characterisation

Plastic size in the suspension containing 25 μg L^{-1} was confirmed by Dynamic Light Scattering (DLS) on a Zeta PALS Zeta Potential Analyzer (Brookhaven Instruments Corporation, USA). Attenuated total reflection-infrared (ATR-IR) spectra were recorded over the wavenumber range 4000−500 cm^{-1} (Jasco FT-IR-4100, USA) to confirm the functional and structural groups. This analysis was performed by using the suspensions containing highest concentration of NPs with Cu. UV–visible absorption spectra were analysed using 1 cm quartz cells (Agilent 8453, USA) to investigate the potential adsorption of Cu onto the NPs. This analysis involved suspensions containing NPs individually, as well as the combination of highest concentration of NPs with Cu. High-Resolution Field Emission Scanning Electron Microscopy (HR-FE-SEM) with Energy Dispersive X-Ray Analysis (EDX; Hitachi SU8010, Japan) was performed to characterise PS NPs surface, and to check the % of elements and further elemental mapping was used to detect Cu adsorbed onto NPs. This analysis involved suspensions containing the lowest concentration of NPs with the highest Cu concentration.

2.4. Intracellular reactive oxygen species

Assessment of ROS was conducted using Mito Red 53271 (Sigma-Aldrich), a dye that produces a red fluorescent compound upon oxidation by intracellular ROS sequestered in the mitochondria. This dye is commonly used to assess mitochondrial status in response to various stress conditions (Azevedo et al., 2009; Pradhan et al., 2015). To prepare the samples, mycelia were washed in phosphate-buffered saline (PBS; pH 7.4) and incubated with Calcofluor White Reagent (1 min; Fluka Analytical) to stain the fungal cell wall. Subsequently, the mycelia were washed in PBS followed by incubation with MitoRed (10 mg mL^{-1}, 30 min) at room temperature in the dark. Stained mycelia were placed on a μ-slide 8 well (Ibidi GmbH, Germany) and scanned under a confocal microscope (Carl Zeiss LSM 710, Jena, Germany) equipped with a Plan-Apochromat 63′/1.4 oil objective and lasers Diode 405–30 and DPSS561-10 (Fernandes et al., 2014). Quantification of fluorescence was performed using automated settings in the laser scanning confocal microscope and was analysed by using Fiji/ImageJ software (Schneider et al., 2012). Parameters such as selection of the region of interest (ROI), filtering background noise, focus and threshold intensity were set to avoid excessive or weak signal. All quantitation and analysis were performed using three images per treatment (Amaldoss et al., 2022; Deshpande et al., 2021). All treatments (n = 21) encompassing control, NPs and Cu individually and all their combinations were assessed.

2.5. Plasma membrane integrity

Plasma membrane integrity in response to NPs and metals was evaluated using propidium iodide (94% HPCL; Sigma-Aldrich). This dye is commonly employed to distinguish between early and late stages of apoptosis, as it is unable to penetrate the cell unless the plasma membrane is compromised (Pradhan et al., 2015). Therefore, mycelia exhibiting intense red fluorescence were indicative of plasma membrane disruption. Briefly, after washing the mycelia with PBS, fungal cell wall was stained using Calcofluor White Reagent. Mycelia were again washed with PBS and then incubated with propidium iodide (5 mg mL^{-1}) for 15 min at room temperature in the dark. Stained mycelia were placed on a μ-slide 8 well (Ibidi GmbH, Germany) and scanned under a confocal microscope and quantified (Brazill et al., 2018) as described above. All treatments (n = 21) encompassing control, NPs and Cu individually and all possible combinations were evaluated.

2.6. Fungal biomass

Initial weight of filter papers (Millipore 0.5 μm, 0.45 mm) were determined after subjecting them to freezing and lyophilisation process

(−50 °C, 12 h, Lablyo mini, UK). Suspensions were subsequently filtered through pre-weighed filter papers, which were then frozen, lyophilised, and weighed to the nearest 0.001 g in order to quantify fungal biomass. In addition, replicates containing only media were filtered and weighed to ensure that the weight of fungal biomass was not influenced by the media. Fungal biomass serves as a proxy for fungal growth, reflecting overall increases or decreases in mycelial mass.

2.7. Statistical analyses

Intracellular ROS production, plasma membrane disruption and fungal biomass were assessed by one-way factorial permutational multivariate analysis of variance (PERMANOVA, $\alpha \leq 0.05$) with treatments as a factor (Amaldoss et al., 2022; Deshpande et al., 2021). Matrices of similarity were based on Bray-Curtis similarity with 9999 permutations and Type III sums of squares (Anderson, 2017; Anderson et al., 2008). To evaluate significant differences on ROS production and plasma membrane disruption between treatments, Monte Carlo sampling ($p \leq 0.05$; Anderson and Robinson, 2003) was employed to derive p-values, considering the limited number of possible permutations. Furthermore, to assess the significant differences on biomass production between treatments, pairwise test ($p \leq 0.05$) was used (Anderson et al., 2008). PERMANOVA is a non-parametric test especially suited when assumptions of a parametric ANOVA are not met (Anderson et al., 2008). These analyses were performed in Primer v6.1.13 (Clarke and Gorley, 2006) with PERMANOVA + v.1.0.3 add-on (Anderson et al., 2008).

3. Results

3.1. Characterisation of NPs

DLS data revealed that both the bare and –COOH NPs in the stock suspension exhibited a mean size of 74 ± 8.9 and 81 ± 9.4 nm, respectively. This indicates that the suspensions were effectively dispersed exhibiting minimal or negligible agglomeration (Gao et al., 2022). FTIR spectra represent the asymmetric and symmetric stretching bands at 2976–2808 cm^{-1}, confirming the presence of methylene ($–CH_2$) groups in all the samples analysed (Fig. 1). Notably, FTIR spectra of control and the treatment containing bare NPs and Cu showed broad spectral bands at 3411–3371 cm^{-1} (hydroxyl group; –OH), 1643 cm^{-1} (carbonyl group; C═O groups), and sharp bands at 1100–1041 cm^{-1} (C–O bonds) (Seena et al., 2022a); whereas all these peaks decreased in suspension containing –COOH NPs and Cu. The absorption maxima observed at 326 nm in the UV–visible spectra (Fig. 2) can be attributed to π–π* transition. Notably, absorption peaks of the suspensions decreased gradually with the presence of –COOH functional group and Cu, suggesting an increase in adsorption of Cu. FE-SEM images of the suspensions with the highest concentrations of bare NPs combined with Cu revealed a nonporous, smooth membranous phase (Kumar and Koh, 2014) and was different when compared to control and the other –COOH NPs counterpart (Fig. 3a–c). The sample with –COOH NPs evidenced dome shaped cavity and non-porous surface whereas the control showed microfibrils (Kumar and Koh, 2014). Moreover, SEM EDX analysis demonstrated a higher Cu percentage (0.77%) in suspensions containing –COOH with Cu, in contrast to the control (0%) and bare NPs with Cu (0.22%) (Figs. S2a–c).

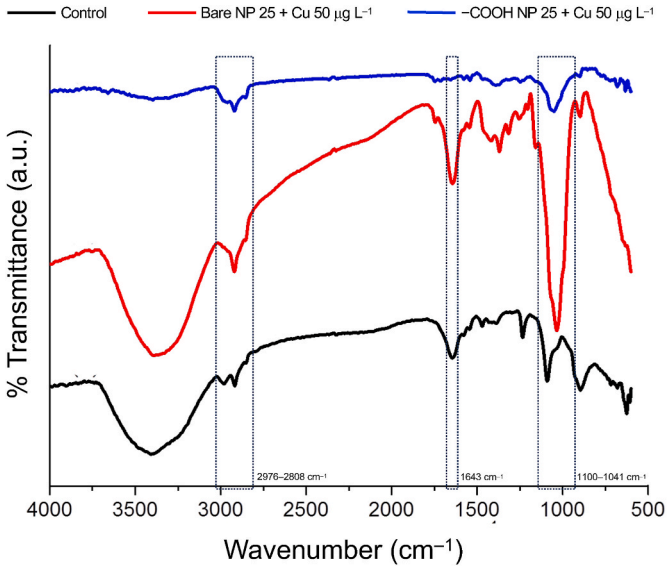

Fig. 1. Fourier-Transform Infrared (FTIR) spectroscopy of suspensions comprising control, highest concentrations of bare and functionalised (–COOH) nanoplastics (NPs) with highest copper (Cu) concentration.

3.2. Intracellular reactive oxygen species

In control group (0 μg L^{-1} NPs and Cu), lack of red fluorescence, observed after staining mycelia with MitoRed, indicated the absence of intracellular accumulation of ROS (Fig. 4a–d). Moreover, there was a progressive enhancement in red fluorescence with increasing exposure concentrations. Consistent with observations in the confocal microscopy images, control group exhibited the lowest accumulation of ROS as confirmed by the quantification of fluorescence intensity derived from the confocal microscopy images (Fig. 5a). Whereas all the other treatments exhibited a NPs concentration-dependent pattern (one-way PERMANOVA; $F_{20,42} = 18.747$, $p = 0.0001$). Control group showed significant differences from all treatments (pairwise test; $p = 0.0001$ to 0.0048); on average, all treatments displayed ~65% higher accumulation of ROS compared to control group. Additionally, significant differences were observed between the two Cu concentrations (25 and 50 μg L^{-1}; $p = 0.006$; Table 1) and between all the tested bare NPs concentrations (up to 25 μg L^{-1}; $p = 0.0031$ to 0.0456). The highest concentration of Cu (50 μg L^{-1}) resulted in an increase (by 25%) in ROS accumulation compared to all treatments involving bare NPs. However, significant differences were only observed between the treatment containing bare NPs (0.25 and 2.5 μg L^{-1}) and Cu (50 μg L^{-1}) and combinations of bare NPs (0.25 and 2.5 μg L^{-1}) with Cu at concentrations of 25 and 50 μg L^{-1} ($p = 0.0001$ to 0.0122; Table 1). In general, treatments containing –COOH NPs were found to be more harmful, leading to an increase (by 25%) in ROS accumulation compared to bare NPs (Fig. 5a). The highest concentration of –COOH NPs (25 μg L^{-1}) exhibited a more

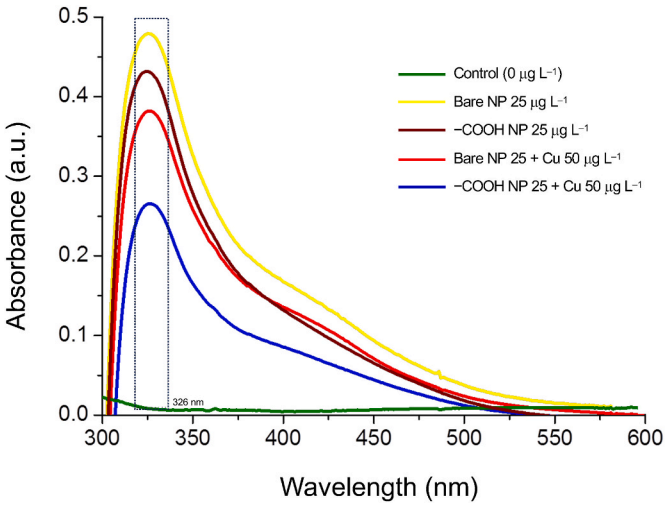

Fig. 2. UV–visible spectra of suspensions consisting of control, highest concentration of bare and functionalised (–COOH) nanoplastics (NPs) individually as well as with highest copper (Cu) concentration.

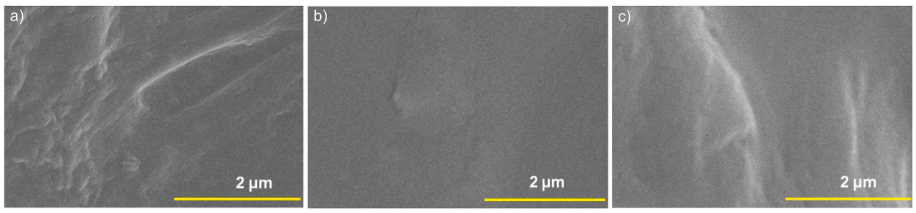

Fig. 3. Field Emission Scanning Electron Microscopy (FE-SEM) images of the suspension constituting (a) control, (b) lowest concentration of bare nanoplastics (NPs) with highest copper (Cu) concentration and (c) lowest concentration of functionalised (–COOH) NPs along with highest concentration of Cu at magnifications 2 µm and 5kV × 25 k.

detrimental effect (respectively by 22 and 14%) compared to the highest concentration of Cu (50 µg L^{-1}), as well as –COOH NPs with Cu (50 µg L^{-1}). However, significant differences were only observed between the highest concentration of –COOH NPs (25 µg L^{-1}) and Cu (25 µg L^{-1}; $p = 0.0009$ and 50 µg L^{-1}; $p = 0.0473$).

3.3. Plasma membrane integrity

Plasma membrane disruption was absent in fungi exposed to control group, as indicated by the lack of red fluorescence after staining with propidium iodide (Fig. 4e–h). Furthermore, there was a progressive rise in red fluorescence as the exposure concentrations increased (Fig. 4e–h). In accordance to confocal microscopy images, control group displayed minimal occurrence of plasma membrane damage as visualised by the quantification of fluorescence intensity (Fig. 5b). Although fungal plasma membrane disruption was significantly different among treatments (one-way PERMANOVA; $F_{20,42} = 10.294$, $p = 0.0001$; Table 2), dose-dependent response was absent (Fig. 5b). However, significant differences were noted between control and all other treatments ($p = 0.0001$ to 0.0043) except for treatments containing Cu (25 and 50 µg L^{-1}; pairwise test; $p \geq 0.05$). The highest concentration of Cu (50 µg L^{-1}) elicited a greater detrimental effect compared to its lowest concentration (25 µg L^{-1}), leading to an increase (by 23%) in plasma membrane disruption ($p \geq 0.05$; Table 2). Nonetheless, both Cu concentrations were less harmful (by ~50%) than all the other treatments excluding control. Notably, only the lowest Cu concentration exhibited significant differences compared to all treatments involving PSNP types individually or with Cu ($p = 0.0006$ to 0.0296; Table 2). Both types of PS NPs, individually at all tested concentrations (up to 25 µg L^{-1}), did not exhibit significant differences from each other. Plasma membrane disruption was more prominent when the fungi were exposed to treatments containing PS NPs (2.5 and 25 µg L^{-1}) with the highest Cu concentration. However, treatments containing –COOH with Cu exhibited the highest level of plasma membrane disruption, but these treatments did not show significant differences compared to certain other treatments (see Table 2).

3.4. Fungal biomass

Fungal biomass production was significantly influenced by PS NP types, metals, and their combinations at all tested concentrations (one-way PERMANOVA; $F_{20,155} = 14.381$; $p = 0.0001$; Fig. 5c). Notably, a dose-dependent response was not observed. Additionally, no significant differences were found between the Cu concentrations (pairwise test; $p > 0.05$; Table 3) and between concentrations of all the tested PS NP types ($p > 0.05$). Interestingly, exposure to Cu at 25 µg L^{-1} ($p < 0.05$) and 50 µg L^{-1} ($p = 0.0102$; Table 3) resulted in increased (respectively by 12 and 16%) biomass production compared to control group. Additionally, exposure to bare NPs and their combinations with Cu resulted in increased biomass production (up to 19%), except for bare NPs (2.5 and 25 µg L^{-1}) with the highest Cu concentration (Fig. 5c). However, these effects were not significantly different from the control group ($p > 0.05$; Table 3). On the other hand, fungal exposure to treatments containing –COOH NPs suppressed their growth (by 16%; $p = 0.0003$ to 0.012) compared to the control group.

4. Discussion

Aquatic hyphomycetes are crucial components of freshwater food webs as they decompose plant material, thereby releasing nutrients that can be utilised by other organisms in the ecosystem. The role of these fungi in nutrient cycling and organic matter decomposition is critical for the functioning of freshwater ecosystems (Barros and Seena, 2022; Seena et al., 2022b). Aquatic hyphomycetes are sensitive to a variety of anthropogenic stressors that can negatively impact their growth and decomposition activities. Among these stressors, metals such as Cu is a prevalent metal pollutant known for its toxic effects on these fungi. The fungal cell wall harbours negatively charged locations, including glucuronic acid, which is capable of binding metal ions (Krauss et al., 2011; Braha et al., 2007).

The impact of plastics, especially functionalised NPs, on aquatic fungi is an emerging field. Recurrent detection of PS in freshwater ecosystems (Li et al., 2020; Wagner et al., 2014) emphasises the urgency for in-depth exploration of the ecological implications and effects of plastics, including PS NPs. Furthermore, in freshwater systems where NPs and Cu coexist, NPs may have the capacity to modulate the toxicity of Cu (Wan et al., 2021). Notably, NPs can enhance the uptake of Cu by aquatic organisms, influencing their toxicity levels (Bellingeri et al., 2019). In addition, NPs have been identified as potential carriers of Cu facilitating its transportation and accumulation in aquatic organisms (Della Torre et al., 2014; Koelmans et al., 2013). These compelling findings emphasise the importance of extensive investigations to comprehend the ecological impacts of co-occurring Cu and NPs in aquatic systems, considering environmentally realistic concentrations. In this pioneering study, a comprehensive examination was conducted to assess the cellular and physiological responses of the ubiquitous aquatic hyphomycete ARTE to environmentally relevant concentrations of bare and functionalised (–COOH) PS NPs and Cu, individually and all possible combinations. Overall, the results provided evidence that ARTE exhibited heightened accumulation of ROS and disruption of plasma membrane upon exposure to increasing concentrations of both types of PS NPs, whether individually or with Cu. Furthermore, adsorption of Cu onto NPs was detected, and their co-exposure intensified the negative effects particularly leading to plasma membrane disruption. However, it is noteworthy that these findings only partially support the hypotheses, as the observed impact on ROS accumulation and fungal growth did not align with the anticipated trends.

4.1. Characterisation

Although Cu plays a vital role in several biological processes, its high concentrations can pose a significant threat, especially in aquatic systems, where it is more bioavailable (Keller et al., 2017). Besides, Cu can be easily adsorbed by NPs through mechanisms such as electrostatic attraction, ion exchange and surface complexation mechanisms (Chen et al., 2022). Adsorption of Cu onto NPs is influenced by various factors,

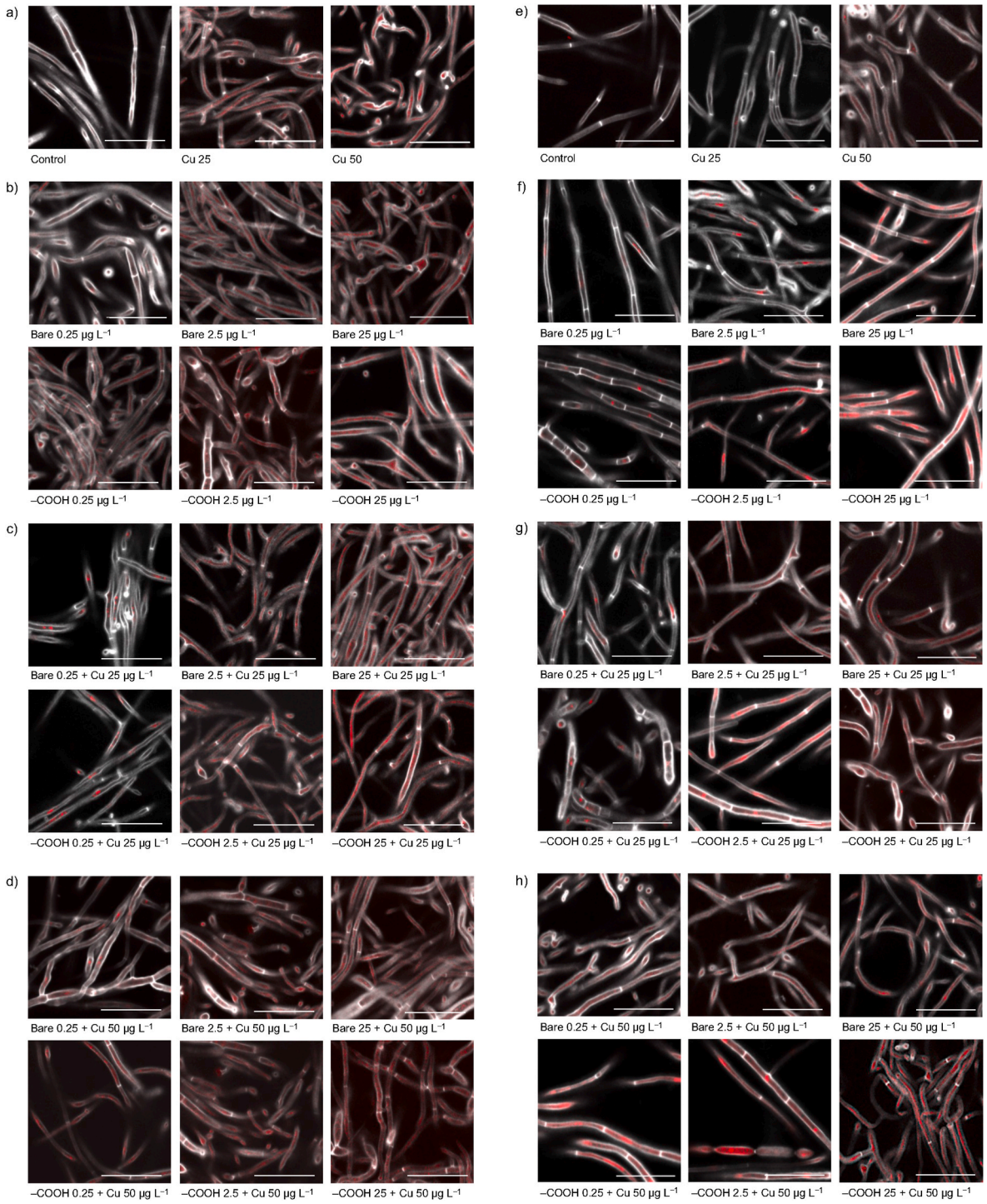

Fig. 4. Confocal microscopy images of (a–d) reactive oxygen species (ROS) accumulation and (e–h) plasma membrane disruption in the suspensions containing control as well as bare and functionalised (–COOH) nanoplastics (NPs) and copper (Cu) individually and in all possible combinations arranged in the increasing order of exposure concentrations.

including the properties of NPs such as surface functionalisation. In this study, a reduction in the intensity of peaks in the FTIR spectra, specifically in the suspension containing –COOH NPs (25 μg L^{-1}) with Cu (50 μg L^{-1}) was observed indicating the occurrence of electrostatic attraction (Chen et al., 2022). This mechanism is anticipated to occur when negatively charged NPs, such as –COOH, attract positively charged Cu ions, resulting in their adsorption onto the surface of NPs. Furthermore, UV-absorption spectra of the aforementioned suspension exhibited a significant decrease compared to control and suspension containing bare NPs with Cu. Elemental mapping also confirmed adsorption of Cu onto NPs surface; concentration of Cu was more in suspension containing –COOH NPs and Cu. FE-SEM analysis of the sample containing bare NPs with Cu indicated that fungal mycelia were embedded in the NPs leading to a nonporous smooth surface. Whereas the presence of –COOH groups in the other NPs sample resulted in a dome-shaped cavity with mycelia also embedded within these NPs, leading to a nonporous surface. Additionally, in the control group devoid of NPs, mycelia exhibited the formation of microfibrils.

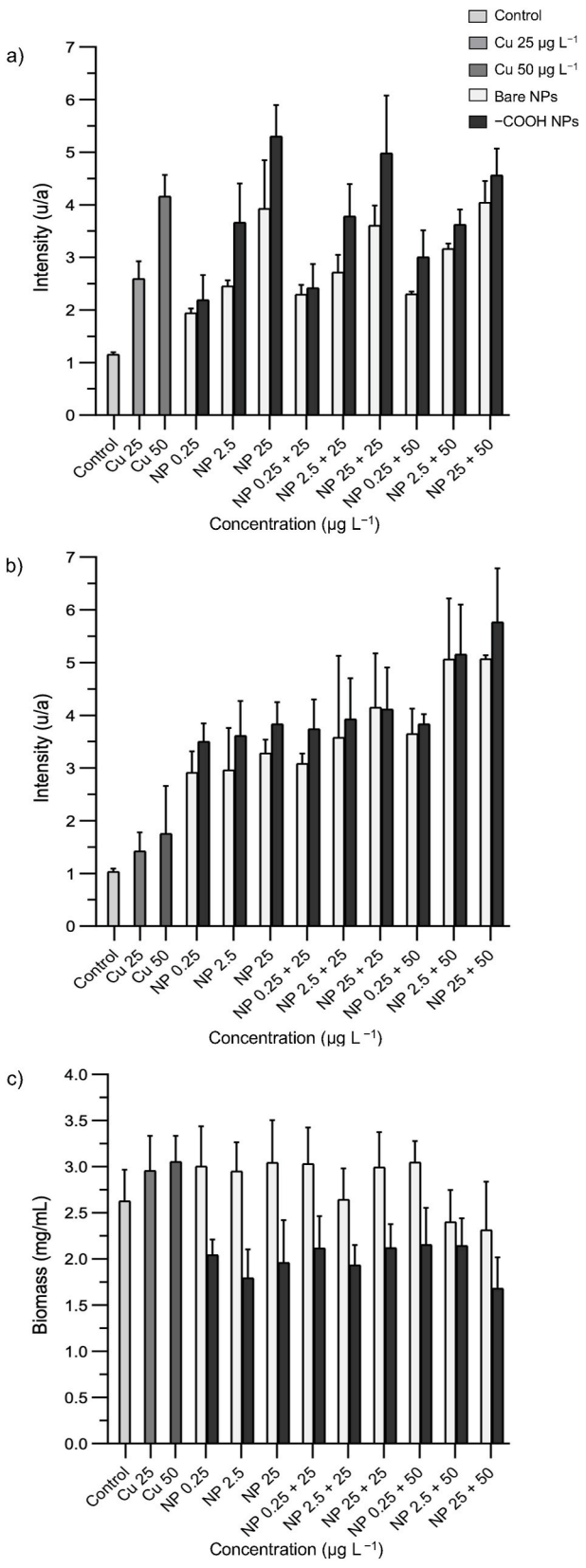

Fig. 5. Fluorescence intensity of the confocal microscopy images of (a) reactive oxygen species (ROS) accumulation and (b) plasma membrane disruption as well the (c) fungal biomass production (growth) derived from the suspensions containing control as well as bare and functionalised (–COOH) nanoplastics (NPs) and copper (Cu) individually and in all possible combinations arranged in the increasing order of exposure concentrations.

4.2. Cellular responses

The study revealed that treatments involving PS NPs with carboxyl (–COOH) functional groups were more detrimental to ARTE compared to treatments with bare NPs. This suggests that the –COOH groups can modulate the negative impacts on these aquatic fungi. For example, adsorption of positively charged ($–NH_2$) PS NPs by algae such as *Chlorella* and *Scenedesmus* (primary producers) was greater than negatively charged (–COOH) PS NPs. However, both types of NPs caused inhibition of algal photosynthetic activities and induced the production of ROS in a concentration-dependent manner (Bhattacharya et al., 2010). In addition, exposure to –COOH PS NPs inhibited growth of the algae *Raphidocelis subcapitata*, leading to morphological alterations, disturbance of mitotic cycle and reduction in photosynthetic efficiency (Bellingeri et al., 2019). Functionalisation of NPs play a crucial role in shaping their toxic mechanisms (Zhang et al., 2022a,b). In general, charged NPs produces increased levels of ROS, triggering oxidative stress, alterations in membrane permeability, and disruption of cellular function (Zhang et al., 2022a,b). Additionally, they may have the potential to induce cell apoptosis (Qu et al., 2023).

Studies exploring the interactions between charged NPs and fungi are limited. Diverse functional groups of the fungal cell wall (Gadd and Sayer, 2000), may interact with charged NPs, potentially resulting in their adsorption onto fungal cell surface. Given the research carried out on eukaryotic cells like animal or human cells (for review see, Zhang et al., 2022a,b), it's reasonable to consider that fungi might also have various mechanisms for internalising NPs into lysosomes (Xu et al., 2021). For instance, negatively charged NPs may escape from lysosomes and influence cellular components to induce stress (Yang and Wang, 2023), while positive NPs destabilise lysosomes promoting a cascade of cellular damage through ROS generation (Zhang et al., 2022a,b). Furthermore, the formation of the eco-corona is also influenced by the surface charge of NPs (Zhang et al., 2022a,b).

The current study revealed that the treatment consisting of lower concentrations of both NPs with Cu effectively mitigated the accumulation of ROS, which was in contrast to the treatment containing the highest concentration of Cu. Importantly, the highest concentration of –COOH, either individually or in combination with Cu, significantly contributed to the increased accumulation of ROS. In addition, it is noteworthy that enhanced plasma membrane disruption caused by exposure to NPs with Cu was observed at all concentrations, highlighting the adverse effects of this combination compared to Cu individually. This observation prompts further investigation into the underlying mechanisms for overall cellular health and function. Previous studies have provided evidence that combined exposure to microplastics and metals influenced their impact on organisms. For instance, combination of microplastics (polymer of undisclosed composition, 2 mg L^{-1}) and Cu (60 and 125 µg L^{-1}) had a greater effect on biomarkers, such as ROS, lipid peroxidation, superoxide dismutase and glutathione on zebrafish larvae (Santos et al., 2021). This indicated that microplastics may serve as a vector for metal uptake leading to reduced survival and growth (Santos et al., 2021). Another study investigating the impact of PS microplastics (1 mg L^{-1}) with Cu (up to 2 mg L^{-1}) on a freshwater fish (*Oreochromis niloticus*), revealed that their exposure increases Cu bioaccumulation and results in histopathological changes in the liver, intestine and gills (Zhang et al., 2022). In a previous study, exploring the co-exposure of various types of PS NPs (up to 100 mg L^{-1}) with Cu (1.5 mg L^{-1}), an increased level of oxidative damage to marine green algae (*Platymonas helgolandica*) was observed. Interestingly, adsorption of Cu onto PS NPs was not detected, yet the presence of PS NPs facilitated the interaction between Cu and algal cells, leading to increased toxicity (Gao et al., 2022). This suggests that the mechanism of combined toxicity between NPs and metals may not solely involve direct adsorption, but also indirect interactions between these pollutants and organisms (Gao et al., 2022).

Table 1
Post hoc pairwise PERMANOVA comparisons of reactive oxygen species production (ROS). Upper diagonal = p values. Lower diagonal = t values.

				Bare NP			Bare NP + Cu 25			Bare NP + Cu 50			−COOH NP			−COOH NP			−COOH NP		
	Control (μg L^{-1})	Cu 25	Cu 50	0.25	2.5	25	0.25	2.5	25	0.25	2.5	25	0.25	2.5	25	0.25	2.5	25	0.25	2.5	25
Control		**0,0008***	**0,0001***	**0,0002***	**0,0002***	**0,0005***	**0,0003***	**0,0002***	**0,0001***	**0,0001***	**0,0001***	**0,0002***	**0,0048***	**0,0002***	**0,0001***	**0,0017***	**0,0004***	**0,0002***	**0,0001***	**0,0002***	**0,0001***
Cu 25	10,3540		**0,0060***	**0,0169***	0,5268	0,0565	0,2226	0,6759	**0,0245***	0,1798	**0,0482***	**0,0064***	0,2576	0,0621	**0,0009***	0,5931	**0,0370***	**0,0140***	0,2958	**0,0168***	**0,0030***
Cu 50	18,1980	5,0335		**0,0001***	**0,0006***	0,6476	**0,0014***	**0,0091***	0,1633	**0,0007***	**0,0122***	0,7484	**0,0055***	0,3506	**0,0473***	**0,0098***	0,4329	0,3229	**0,0397***	0,1402	0,3569
Bare NP																					
0.25	14,9820	3,7648	11,2450		**0,0040***	**0,0047***	**0,0379***	**0,0132***	**0,0006***	**0,0044***	**0,0002***	**0,0003***	0,4169	**0,0061***	**0,0003***	0,1374	**0,0022***	**0,0018***	**0,0096***	**0,0002***	**0,0004***
2.5	22,0740	0,6806	8,0054	6,3290		**0,0263***	0,2700	0,2796	**0,0059***	0,0810	**0,0005***	**0,0012***	0,3584	**0,0302***	**0,0004***	0,8226	**0,0163***	**0,0090***	0,1201	**0,0012***	**0,0012***
25	8,0134	2,6018	0,5153	4,8721	3,2726		**0,0180***	0,0753	0,6488	**0,0178***	0,2135	0,7739	**0,0267***	0,7487	0,1005	**0,0465***	0,8981	0,2776	0,1929	0,6781	0,3379
Bare NP + Cu 25																					
0.25	12,9040	1,4154	7,6761	3,0834	1,3047	3,5996		0,1263	**0,0051***	0,9293	**0,0026***	**0,0010***	0,6656	**0,0161***	**0,0003***	0,7305	**0,0110***	**0,0043***	0,0620	**0,0024***	**0,0006***
2.5	10,5940	0,4507	4,4794	4,2474	1,2557	2,2935	1,9138		**0,0423***	0,0930	0,1046	**0,0095***	0,1853	0,1001	**0,0020***	0,4042	0,0525	**0,0170***	0,4656	**0,0242***	**0,0054***
25	15,9910	3,4836	1,6882	8,9762	5,6885	0,4972	5,7528	2,9532		**0,0019***	0,1144	0,2412	**0,0176***	0,9434	**0,0097***	**0,0318***	0,7180	0,1113	0,1691	0,9365	0,0593
Bare NP + Cu 50																					
0.25	28,3710	1,6169	9,5796	5,8081	2,3085	3,7823	0,1110	2,1914	7,0688		**0,0001***	**0,0009***	0,6186	**0,0159***	**0,0001***	0,7405	**0,0083***	**0,0036***	0,0510	**0,0006***	**0,0009***
2.5	34,2310	2,7609	4,3784	14,7540	8,0236	1,4750	6,3809	2,0795	1,9962	14,5460		**0,0148***	**0,0324***	0,3110	**0,0018***	0,0693	0,1610	0,0371	0,5649	0,0560	**0,0053***
25	18,1020	4,7665	0,3457	10,9830	7,6753	0,3327	7,3881	4,2108	1,3619	9,2613	3,9706		**0,0085***	0,4577	**0,0308***	**0,0116***	0,5623	0,2574	0,0535	0,2175	0,2492
−COOH NP																					
0.25	5,0330	1,2809	4,7365	0,9096	1,0578	3,1134	0,4692	1,5946	3,7120	0,5467	3,1386	4,5545		**0,0349***	**0,0031***	0,5795	**0,0230***	**0,0088***	0,0912	**0,0150***	**0,0043***
2.5	8,8687	2,4627	1,0521	5,1357	3,2623	0,3549	3,6230	2,1137	0,1170	3,8686	1,1669	0,8365	3,0201		**0,0456***	0,0551	0,8388	0,1639	0,2684	0,9398	0,1642
25	19,1570	7,1717	2,7725	13,3630	10,6200	2,1054	9,9681	6,6343	4,3029	12,1190	7,5555	3,1150	6,2005	2,8312		**0,0023***	**0,0417***	0,6530	**0,0069***	**0,0075***	0,1820
−COOH NP + Cu 25																					
0.25	6,1916	0,5887	4,2720	1,8448	0,2717	2,6727	0,3783	0,9256	3,1650	0,3811	2,4844	4,0730	0,6149	2,5357	5,8780		**0,0357***	**0,0138***	0,2018	**0,0250***	**0,0077***
2.5	10,5670	3,0314	0,8707	6,2652	4,1205	0,1748	4,4412	2,6370	0,3831	4,8576	1,7106	0,6264	3,4599	0,2386	2,8791	2,9684		0,1946	0,1628	0,7504	0,1813
25	8,9317	3,9849	1,1265	6,1954	4,7623	1,2313	4,9956	3,6911	2,0486	5,2469	3,1171	1,3164	4,2222	1,6611	0,5025	3,8589	1,5601		**0,0389***	0,1027	0,6394
−COOH NP + Cu 50																					
0.25	9,2804	1,2212	2,9577	4,3866	2,0145	1,5552	2,5191	0,8220	1,6613	2,7602	0,6334	2,7162	2,0980	1,2944	4,9130	1,5095	1,6768	2,9074		0,1382	**0,0208***
2.5	20,3680	3,9265	1,8184	11,2520	7,2142	0,4753	6,8063	3,3282	0,0946	9,2905	2,6812	1,4511	3,9447	0,1244	4,7300	3,3937	0,3511	2,0824	1,8465		**0,0487***
25	17,1390	5,6441	1,0304	11,2170	8,3841	1,1012	8,1052	5,1229	2,5873	9,7257	5,2014	1,3589	5,2017	1,7000	1,6262	4,7894	1,6021	0,5161	3,6133	2,7966	

*significantly different ($p < 0.05$) based on Monte Carlo simulation.

Table 2
Post hoc pairwise PERMANOVA comparisons of plasma membrane disruption. Upper diagonal = p values. Lower diagonal = t values.

				Bare NP			Bare NP + Cu 25			Bare NP + Cu 50			−COOH NP			−COOH NP			−COOH NP		
	Control (μg L^{-1})	Cu 25	Cu 50	0.25	2.5	25	0.25	2.5	25	0.25	2.5	25	0.25	2.5	25	0.25	2.5	25	0.25	2.5	25
Control		0,0978	0,1945	**0,0002***	**0,0011***	**0,0001***	**0,0001***	**0,0043***	**0,0008***	**0,0003***	**0,0002***	**0,0001***	**0,0001***	**0,0005***	**0,0001***	**0,0001***	**0,0002***	**0,0003***	**0,0001***	**0,0001***	**0,0001***
Cu 25	2,1167		0,6655	**0,0092***	**0,0201***	**0,0034***	**0,0045***	**0,0296***	**0,0069***	**0,0038***	**0,0026***	**0,0006***	**0,0026***	**0,0053***	**0,0023***	**0,0046***	**0,0033***	**0,0033***	**0,0015***	**0,0010***	**0,0009***
Cu 50	1,5692	0,4970		0,1125	0,1455	0,0625	0,0828	0,1256	**0,0448***	0,0511	**0,0224***	**0,0169***	0,0578	0,0615	**0,0354***	**0,0463***	**0,0409***	**0,0363***	**0,0400***	**0,0168***	**0,0096***
Bare NP																					
0.25	11,2290	4,4100	1,9847		0,9241	0,2568	0,5312	0,5728	0,1224	0,1186	**0,0275***	**0,0009***	0,1303	0,2038	0,0519	0,1058	0,0929	0,0625	**0,0240***	**0,0130***	**0,0063***
2.5	6,2209	3,3881	1,7643	0,1349		0,4525	0,6731	0,6326	0,1971	0,2492	0,0596	**0,0191***	0,3016	0,3233	0,1622	0,2195	0,1904	0,1390	0,1341	**0,0371***	**0,0190***
25	18,3280	5,5526	2,4302	1,3489	0,8236		0,3662	0,8071	0,2479	0,3346	0,0537	**0,0010***	0,4424	0,5030	0,1207	0,2777	0,2283	0,1355	**0,0427***	**0,0208***	**0,0073***
Bare NP + Cu 25																					
0.25	19,9600	5,2905	2,2521	0,7039	0,4579	1,0448		0,6969	0,1567	0,1390	**0,0294***	**0,0003***	0,1411	0,2722	**0,0437***	0,1298	0,1162	0,0713	**0,0096***	**0,0126***	**0,0049***
2.5	4,3606	2,9072	1,8108	0,6326	0,5384	0,3305	0,4744		0,5598	0,7396	0,2483	0,1623	0,8006	0,8092	0,6191	0,6909	0,6157	0,5164	0,5892	0,1943	0,1186
25	7,5717	4,6700	2,6498	1,9255	1,5442	1,3431	1,7448	0,6589		0,5509	0,4040	0,2242	0,4081	0,5563	0,7182	0,6386	0,8209	0,9647	0,7111	0,3011	0,1451
Bare NP + Cu 50																					
0.25	12,8430	5,5554	2,6480	1,9839	1,3319	1,0961	1,8438	0,4066	0,6653		0,1277	**0,0113***	0,7269	0,9218	0,6405	0,8513	0,6614	0,4528	0,5443	0,0676	**0,0236***
2.5	8,9554	5,5990	3,1996	3,2102	2,5199	2,7328	3,1778	1,3470	0,9388	1,8992		0,8470	0,0842	0,1407	0,1706	0,1589	0,2493	0,3350	0,1481	0,9039	0,4803
25	38,5030	8,2932	3,7445	6,9756	3,6833	9,2102	12,8740	1,6976	1,4411	4,1323	0,2378		**0,0035***	**0,0312***	**0,0128***	**0,0262***	0,0757	0,1043	**0,0004***	0,9029	0,3247
−COOH NP																					
0.25	16,3100	5,7440	2,5997	1,9089	1,1891	0,8631	1,8267	0,3423	0,9314	0,3816	2,2618	6,3290		0,8389	0,3552	0,5894	0,4505	0,2843	0,2102	**0,0374***	**0,0143***
2.5	9,4586	4,8990	2,4955	1,5248	1,1277	0,7331	1,2704	0,3285	0,6640	0,1151	1,7738	3,0795	0,2161		0,6403	0,8060	0,6547	0,4693	0,5670	0,0884	**0,0323***
25	15,8210	6,1079	2,8470	2,7020	1,7070	1,9319	2,8807	0,5876	0,4027	0,5072	1,6676	4,3265	1,0343	0,5135		0,8146	0,9140	0,6566	0,9471	0,0865	**0,0270***
−COOH NP + Cu 25																					
0.25	11,7320	5,4812	2,6836	2,0574	1,4261	1,2395	1,9143	0,4667	0,5097	0,2038	1,6952	3,3972	0,5807	0,2655	0,2527		0,8002	0,5673	0,7573	0,0932	**0,0342***
2.5	10,1110	5,3016	2,7276	2,1272	1,5563	1,4085	1,9741	0,5762	0,2617	0,4904	1,3586	2,4290	0,8414	0,5052	0,1422	0,2956		0,7704	0,8957	0,1638	0,0650
25	10,6550	5,5725	2,8703	2,5177	1,8232	1,8467	2,4384	0,7433	0,0915	0,8520	1,1139	2,0590	1,2477	0,8166	0,5021	0,6367	0,3083		0,6149	0,2247	0,0885
−COOH NP + Cu 50																					
0.25	26,5970	6,6686	2,9365	3,3672	1,8663	2,9299	4,7258	0,6308	0,4240	0,6684	1,7827	9,6515	1,4635	0,6187	0,0871	0,3499	0,1686	0,5457		0,0654	**0,0235***
2.5	11,4500	6,4040	3,4327	4,0271	2,9381	3,6091	4,2068	1,5261	1,1732	2,4479	0,1466	0,1639	2,9749	2,1985	2,2205	2,1705	1,7249	1,4477	2,4725		0,5150
25	12,4330	6,9379	3,7282	4,9156	3,5398	4,6513	5,2908	1,9332	1,7748	3,3259	0,7629	1,1234	3,9592	2,9401	3,1664	3,0011	2,4743	2,2076	3,5658	0,7269	

*significantly different ($p < 0.05$) based on Monte Carlo simulation.

Table 3
Post hoc pairwise PERMANOVA comparisons of biomass production. Upper diagonal = p values. Lower diagonal = t values.

		Bare NP		Bare NP + Cu 25			Bare NP + Cu 50			–COOH NP			–COOH NP + Cu 25			–COOH NP + Cu 50					
	Control (μg L^{-1})	Cu 25	Cu 50	0.25	2.5	25	0.25	2.5	25	0.25	2.5	25	0.25	2.5	25	0.25	2.5	25	0.25	2.5	25
Control		0,0667	**0,0102***	0,0624	0,0542	0,0583	**0,0357***	0,9498	**0,0441***	**0,0092***	0,1745	0,1182	**0,0001***	**0,0003***	**0,0014***	**0,0061***	**0,0001***	**0,0038***	**0,0155***	**0,0062***	**0,0001***
Cu 25	1,9658		0,5053	0,8326	0,9733	0,7132	0,7018	0,0834	0,8066	0,4885	**0,0053***	**0,0111***	**0,0002***	**0,0001***	**0,0001***	**0,0007***	**0,0001***	**0,0002***	**0,0012***	**0,0015***	**0,0001***
Cu 50	2,9645	0,6775		0,6933	0,4733	0,8350	0,8243	**0,0136***	0,6584	0,9768	**0,0006***	**0,0026***	**0,0001***	**0,0001***	**0,0005***	**0,0001***	**0,0001***	**0,0001***	**0,0003***	**0,0002***	**0,0001***
Bare NP																					
0.25	2,0190	0,2061	0,4091		0,8292	0,8837	0,8840	0,0746	0,9845	0,6886	**0,0069***	**0,0110***	**0,0003***	**0,0001***	**0,0003***	**0,0010***	**0,0001***	**0,0003***	**0,0016***	**0,0006***	**0,0001***
2.5	2,0761	0,0552	0,7185	0,2214		0,7055	0,6980	0,0679	0,8344	0,4635	**0,0061***	**0,0126***	**0,0001***	**0,0001***	**0,0006***	**0,0010***	**0,0001***	**0,0003***	**0,0018***	**0,0005***	**0,0002***
25	2,0952	0,3757	0,2235	0,1697	0,3900		0,9820	0,0689	0,8614	0,8255	**0,0093***	**0,0113***	**0,0002***	**0,0003***	**0,0002***	**0,0008***	**0,0002***	**0,0006***	**0,0018***	**0,0013***	**0,0002***
Bare NP + Cu 25																					
0.25	2,3222	0,3884	0,2357	0,1685	0,4002	0,0593		**0,0441***	0,8684	0,8212	**0,0043***	**0,0088***	**0,0001***	**0,0001***	**0,0002***	**0,0005***	**0,0001***	**0,0002***	**0,0009***	**0,0010***	**0,0001***
2.5	0,1045	1,8402	2,8000	1,9037	1,9385	1,9837	2,1952		0,0627	**0,0091***	0,1486	0,1040	**0,0004***	**0,0001***	**0,0020***	**0,0049***	**0,0003***	**0,0033***	**0,0149***	**0,0084***	**0,0001***
25	2,1887	0,2164	0,4332	0,0520	0,2229	0,1929	0,1770	2,0601		0,6605	**0,0047***	**0,0098***	**0,0001***	**0,0001***	**0,0001***	**0,0005***	**0,0002***	**0,0002***	**0,0008***	**0,0015***	**0,0001***
Bare NP + Cu 50																					
0.25	3,1068	0,6925	0,0511	0,4154	0,7441	0,2381	0,2408	2,9282	0,4383		**0,0004***	**0,0023***	**0,0001***	**0,0002***	**0,0002***	**0,0002***	**0,0001***	**0,0001***	**0,0001***	**0,0005***	**0,0002***
2.5	1,4316	3,1809	4,1859	3,1591	3,2837	3,1536	3,4854	1,5098	3,3828	4,3471		0,5769	**0,0196***	**0,0010***	**0,0359***	0,1089	**0,0069***	0,0915	0,1743	0,1380	**0,0004***
25	1,6625	2,9680	3,6390	2,9736	2,9655	2,9299	3,2027	1,7196	3,1185	3,7199	0,5709		0,2296	**0,0345***	0,1965	0,4349	0,0918	0,4224	0,5531	0,5062	**0,0113***
–COOH NP																					
0.25	4,8075	6,8590	9,4646	6,3543	7,6625	6,2304	7,1030	4,8348	7,1178	10,4160	2,6066	1,2793		0,0630	0,5558	0,6689	0,2593	0,5171	0,5604	0,4896	**0,0090***
2.5	4,8269	6,1621	7,2039	5,9893	6,2111	5,7832	6,3630	4,8610	6,3228	7,4165	3,4460	2,2837	1,8966		0,5259	0,0851	0,3428	**0,0345***	0,0702	**0,0303***	0,5371
25	3,0945	4,2002	4,8173	4,1700	4,1343	4,0357	4,3918	3,1367	4,3287	4,8995	2,0798	1,3272	0,7462	0,6774		0,4574	0,9219	0,3788	0,3917	0,3735	0,2552
–COOH NP + Cu 25																					
0.25	3,1312	4,7004	5,8240	4,5705	4,8321	4,4703	4,9503	3,1846	4,8863	6,0510	1,6709	0,7999	0,4483	1,8226	0,8216		0,2589	0,8985	0,8872	0,8533	**0,0240***
2.5	5,1345	6,9120	8,8366	6,5236	7,3758	6,3524	7,1396	5,1620	7,1336	9,4016	3,2041	1,8245	1,1840	1,0266	0,3297	1,1864		0,1364	0,2204	0,1368	0,1077
25	3,6001	5,4420	7,1164	5,1793	5,8121	5,0824	5,7076	3,6508	5,6650	7,5680	1,8171	0,8177	0,6865	2,1482	0,9835	0,1574	1,5727		0,8947	0,9191	**0,0071***
–COOH NP + Cu 50																					
0.25	2,7377	4,2157	5,1682	4,1350	4,2860	4,0470	4,4608	2,7928	4,3890	5,3361	1,4007	0,6239	0,6181	1,8825	0,9050	0,1695	1,2902	0,1745		0,9188	**0,0218***
2.5	3,2134	4,9296	6,4588	4,6975	5,2595	4,6109	5,1799	3,2626	5,1368	6,8659	1,5701	0,6730	0,7952	2,0897	0,9825	0,2300	1,5922	0,1346	0,1306		**0,0096***
25	5,2269	6,4431	7,3758	6,2840	6,4305	6,0459	6,6263	5,2569	6,5894	7,5584	3,9451	2,7600	2,5445	0,6453	1,1795	2,3929	1,7115	2,7404	2,4276	2,6324	

*significantly different ($p < 0.05$) based on Monte Carlo simulation.

4.3. Fungal biomass

In this study, Cu exposure led to increased fungal growth, consistent with previous findings on the stimulating effect of Cu on aquatic hyphomycetes (Azevedo and Cássio, 2010; Quainoo et al., 2016). Cu was observed to stimulate the expression of laccase genes in these aquatic fungi, enhancing the production of laccase enzymes involved in lignin degradation and breakdown of phenolic compounds. This stimulation of laccase genes by Cu promotes their growth, highlighting its role as a growth stimulant through laccase gene expression (Pradhan et al., 2014; Solé et al., 2012). Typically, moderate metal levels (6.33 mg L^{-1}) tend to exert a more pronounced negative impact on aquatic fungal reproduction (sporulation) compared to their growth and decomposition capacity (Duarte et al., 2008; Solé et al., 2008). However, at high concentrations (25.4 mg L^{-1}), Cu has been observed to inhibit both the growth and reproduction of diverse aquatic fungal species (Miersch et al., 1997).

Although numerous studies have been conducted to assess the mode of action of Cu in triggering physiological responses in freshwater fungi (for review see Krauss et al., 2011), mechanisms driving the impacts of NPs on freshwater organisms, particularly fungi, are not yet fully elucidated. However, it is worth noting that PS NPs exposure caused a decline in population growth in freshwater algae (*Scenedesmus obliquus*). Additionally, it resulted in reduced growth of the zooplankton *Daphnia magna*, promoting severe reproductive alterations (0.22–103 mg L^{-1}; Besseling et al., 2014). In general, bare PS NPs individually or with the lowest concentration of Cu revealed a substantial augmentation in fungal biomass production. However, the increase did not surpass the enhancement observed with exposure to Cu individually. Previously, when leaf litter fungal community was exposed to PS NPs (up to 100 μg L^{-1}) an increase in biomass was also evidenced (up to 100 μg L^{-1}; Du et al., 2022). Moreover, a filamentous fungus *Geotrichum candidum* when exposed to PS NPs (up to 100 μg L^{-1}), exhibited increased stress tolerance particularly at lower concentrations (1 and 10 μg L^{-1}) and demonstrated hormesis effect on biomass production (Qv et al., 2022).

Notably, this study revealed a significant reduction in fungal biomass upon exposure to –COOH PS NPs, either individually or with Cu. Various studies have raised concerns about the potential negative impacts of functionalised NPs on aquatic organisms, however to our knowledge, none of the earlier studies have investigated the effects of these plastic particles on the growth of aquatic hyphomycetes. Nevertheless, current understanding indicates that –COOH PS NPs were more toxic to brine shrimp (*Artemia franciscana*) larvae. They formed aggregates within the gut, leading to impaired feeding, motility, and moulting behaviours (Bergami et al., 2016). By contrast, in a study involving the exposure of marine algae (*P. helgolandica*) to both bare and –COOH PS NPs, no significant difference in growth was observed between the two NPs types (Gao et al., 2022). Collectively, these results shed new light on the intricate responses of aquatic fungi to these emerging pollutants and contribute to advancing our understanding of their ecological implications in aquatic environments.

5. Conclusions

This study highlights the intricate and diverse nature of the ecotoxicity associated with PS NPs on aquatic organisms. It is well-established that the effects of PS NPs are influenced by various factors, including NP types, concentrations, surface charge, and interactions with other pollutants. Therefore, there is an urgent requirement to comprehensively understand these factors in order to assess and predict the potential ecological impacts of PS NPs. For instance, integrating genomics and molecular biology could equip researchers with profound insights into the modulation of gene expression patterns in response to co-contaminants, thereby deepening our understanding. Moreover, this study emphasises the importance of investigating the impacts of these pollutants at environmentally realistic concentrations to obtain a more precise understanding of their potential effects. Such investigations are essential for effective environmental management and conservation endeavours, aimed at preserving the health and biodiversity of

freshwater ecosystems.

CRediT authorship contribution statement

Juliana Barros: Methodology, Investigation, Formal analysis, Writing – original draft, Writing – review & editing. Santosh Kumar: Methodology, Investigation, Formal analysis, Writing – review & editing. Sahadevan Seena: Conceptualisation, Methodology, Investigation, Formal analysis, Writing – review & editing, Supervision, Project administration and Funding acquisition.

Declaration of generative AI in scientific writing

During the preparation of this work the authors used ChatGPT by OpenAI to improve readability and language. After using this tool, authors reviewed and edited the content as needed and take full responsibility for the content of the publication.

Declaration of competing interest

The authors declare that they have no known competing financial interests or personal relationships that could have appeared to influence the work reported in this paper.

Data availability

Data will be made available on request.

Acknowledgements

This work was funded (2022.03644.PTDC) by the Foundation for Science and Technology (FCT). This study was also supported by FCT under projects granted to MARE (UIDB/04292/2020) and the associate laboratory ARNET (LA/P/0069/2020). SS (IT057-18-7254) and JB (2022.10696.BD) acknowledge the contract.

Appendix A. Supplementary data

Supplementary data to this article can be found online at https://doi.org/10.1016/j.envpol.2023.122549.

References

Aitken, R.J., Chaudhry, M.Q., Boxall, A.B.A., Hull, M., 2006. Manufacture and use of nanomaterials: current status in the UK and global trends. Occup. Med. 56, 300–306. https://doi.org/10.1093/occmed/kql051.

Amaldoss, M.J.N., Pandzic, E., Koshy, P., Kumar, N., Sorrell, C.C., Unnikrishnan, A., 2022. Detection and quantification of nanoparticle-induced intracellular ROS in live cells by laser scanning confocal microscopy. Methods 207, 11–19. https://doi.org/10.1016/j.ymeth.2022.08.005.

Anderson, M.J., 2017. Permutational Multivariate Analysis of Variance (PERMANOVA). Wiley StatsRef: Statistics Reference Online, pp. 1–15. https://doi.org/10.1002/9781118445112.stat07841.

Anderson, M.J., Gorley, R.N., Clarke, K.R., 2008. PERMANOVA+ for PRIMER: Guide to Software and Statistical Methods. Plymouth, UK.

Anderson, M.J., Robinson, J., 2003. Generalized discriminant analysis based on distances. Aust. N. Z. J. Stat. 45, 301–318. https://doi.org/10.1111/1467-842X.00285.

Avery, S.V., 2001. Advances in Applied MicrobiologyLaskin, A.I., Bennett, J.W., Gadd, G. M. (Eds.), In: Metal Toxicity in Yeasts and the Role of Oxidative Stress. Academic Press, pp. 111–142. https://doi.org/10.1016/S0065-2164(01)49011-3.

Azevedo, M.M., Almeida, B., Ludovico, P., Cássio, F., 2009. Metal stress induces programmed cell death in aquatic fungi. Aquat. Toxicol. 92, 264–270. https://doi.org/10.1016/j.aquatox.2009.02.010.

Azevedo, M.M., Cássio, F., 2010. Effects of metals on growth and sporulation of aquatic fungi. Drug Chem. Toxicol. 33, 269–278. https://doi.org/10.3109/01480540903431440.

Barros, J., Seena, S., 2022. Fungi in freshwaters: prioritising aquatic hyphomycetes in conservation goals. Water 14, 605. https://doi.org/10.3390/w14040605.

Bellingeri, A., Bergami, E., Grassi, G., Faleri, C., Redondo-Hasselerharm, P., Koelmans, A. A., Corsi, I., 2019. Combined effects of nanoplastics and copper on the freshwater alga Raphidocelis subcapitata. Aquat. Toxicol. 210, 179–187. https://doi.org/10.1016/j.aquatox.2019.02.022.

Bergami, E., Bocci, E., Vannuccini, M.L., Monopoli, M., Salvati, A., Dawson, K.A., Corsi, I., 2016. Nano-sized polystyrene affects feeding, behavior and physiology of brine shrimp Artemia franciscana larvae. Ecotoxicol. Environ. Saf. 123, 18–25. https://doi.org/10.1016/j.ecoenv.2015.09.021.

Besseling, E., Wang, B., Lürling, M., Koelmans, A.A., 2014. Nanoplastic affects growth of S. Obliquus and reproduction of D. Magna. Environ. Sci. Technol. 48, 12336–12343. https://doi.org/10.1021/es503001d.

Bhattacharya, P., Lin, S., Turner, J.P., Ke, P.C., 2010. Physical adsorption of charged plastic nanoparticles affects algal photosynthesis. J. Phys. Chem. C 114, 16556–16561. https://doi.org/10.1021/jp1054759.

Borowska, M., Jankowski, K., 2023. Basic and advanced spectrometric methods for complete nanoparticles characterization in bio/eco systems: current status and future prospects. Anal. Bioanal. Chem. 415, 4023–4038. https://doi.org/10.1007/s00216-023-04641-7.

Boucher, J., Friot, D., 2017. Primary Microplastics in the Oceans: a Global Evaluation of Sources. IUCN Gland, Switzerland, p. 43. https://doi.org/10.2305/IUCN.CH.2017.01.en.

Braha, B., Tintemann, H., Krauss, G., Ehrman, J., Bärlocher, F., Krauss, G.-J., 2007. Stress response in two strains of the aquatic hyphomycete *Heliscus lugdunensis* after exposure to cadmium and copper ions. Biometals 20, 93–105. https://doi.org/10.1007/s10534-006-9018-y.

Brazill, J.M., Zhu, Y., Li, C., Zhai, R.G., 2018. Quantitative cell biology of neurodegeneration in Drosophila through unbiased analysis of fluorescently tagged proteins using ImageJ. J. Vis. Exp. 138, 58041 https://doi.org/10.3791/58041.

Cummins, K.W., 1973. Trophic relations of aquatic insects. Annu. Rev. Entomol. 18, 183–206. https://doi.org/10.1146/annurev.en.18.010173.001151.

Chen, C., Wei, F., Ye, L., Wang, Y., Long, L., Xu, C., Xiao, Y., Wu, J., Xu, M., He, J., Yang, G., 2022. Adsorption of Cu2+ by UV aged polystyrene in aqueous solution. Ecotoxicol. Environ. Saf. 232, 113292 https://doi.org/10.1016/j.ecoenv.2022.113292.

Cummins, K.W., Klug, M.J., 1979. Feeding ecology of stream invertebrates. Annu. Rev. Ecol. Systemat. 10, 147–172. https://www.jstor.org/stable/2096788.

Della Torre, C., Bergami, E., Salvati, A., Faleri, C., Cirino, P., Dawson, K.A., Corsi, I., 2014. Accumulation and embryotoxicity of polystyrene nanoparticles at early stage of development of sea urchin embryos Paracentrotus lividus. Environ. Sci. Technol. 48, 12302–12311. https://doi.org/10.1021/es502569w.

Deshpande, P., Gogia, N., Chimata, A.V., Singh, A., 2021. Unbiased automated quantitation of ROS signals in live retinal neurons of Drosophila using Fiji/ImageJ. Biotechniques 71, 416–424. https://doi.org/10.2144/btn-2021-0006.

Dong, Z., Zhu, L., Zhang, W., Huang, R., Lv, X., Jing, X., Yang, Z., Wang, J., Qiu, Y., 2019. Role of surface functionalities of nanoplastics on their transport in seawater-saturated sea sand. Environ. Pollut. 255, 113177 https://doi.org/10.1016/j.envpol.2019.113177.

Du, J., Qv, W., Niu, Y., Qv, M., Jin, K., Xie, J., Li, Z., 2022. Nanoplastic pollution inhibits stream leaf decomposition through modulating microbial metabolic activity and fungal community structure. J. Hazard Mater. 424, 127392 https://doi.org/10.1016/j.jhazmat.2021.127392.

Duarte, S., Pascoal, C., Alves, A., Correia, A., Cássio, F., 2008. Copper and zinc mixtures induce shifts in microbial communities and reduce leaf litter decomposition in streams. Freshw. Biol. 53, 91–101. https://doi.org/10.1111/j.1365-2427.2007.01869.x.

Fernandes, C., Anjos, J., Walker, L.A., Silva, B.M.A., Cortes, L., Mota, M., Munro, C.A., Gow, N.A.R., Gonçalves, T., 2014. Modulation of Alternaria infectoria cell wall chitin and glucan synthesis by cell wall synthase inhibitors. Antimicrob. Agents Chemother. 58, 2894–2904. https://doi.org/10.1128/AAC.02647-13.

Ferreira, V., Koricheva, J., Duarte, S., Niyogi, D.K., Guérold, F., 2016. Effects of anthropogenic heavy metal contamination on litter decomposition in streams – a meta-analysis. Environ. Pollut. 210, 261–270. https://doi.org/10.1016/j.envpol.2015.12.060.

Gadd, G.M., Sayer, J.A., 2000. Influence of fungi on the environmental mobility of metals and metalloids. In: Environmental Microbe-Metal Interactions. John Wiley & Sons, Ltd, pp. 237–256. https://doi.org/10.1128/9781555818098.ch11.

Gao, Z., Wang, S., Zhang, Y., Liu, F., 2022. Single and combined toxicity of polystyrene nanoplastics and copper on *Platymonas helgolandica* var. tsingtaoensis: perspectives from growth inhibition, chlorophyll content and oxidative stress. Sci. Total Environ. 829, 154571 https://doi.org/10.1016/j.scitotenv.2022.154571.

Gessner, M.O., Chauvet, E., 2002. A case for using litter breakdown to assess functional stream integrity. Ecol. Appl. 12, 498–510. https://doi.org/10.2307/3060958.

Gessner, M.O., Chauvet, E., Dobson, M., 1999. A perspective on leaf litter breakdown in streams. Oikos 377–384. https://doi.org/10.2307/3546505.

Gigault, J., El Hadri, H., Nguyen, B., Grassl, B., Rowenczyk, L., Tufenkji, N., Feng, S., Wiesner, M., 2021. Nanoplastics are neither microplastics nor engineered nanoparticles. Nat. Nanotechnol. 16, 501–507. https://doi.org/10.1038/s41565-021-00886-4.

Gigault, J., Halle, A. ter, Baudrimont, M., Pascal, P.-Y., Gauffre, F., Phi, T.-L., El Hadri, H., Grassl, B., Reynaud, S., 2018. Current opinion: what is a nanoplastic? Environ. Pollut. 235, 1030–1034. https://doi.org/10.1016/j.envpol.2018.01.024.

González-Fernández, C., Díaz Baños, F.G., Esteban, M.Á., Cuesta, A., 2021. Functionalized nanoplastics (NPs) increase the toxicity of metals in fish cell lines. Int. J. Mol. Sci. 22, 7141. https://doi.org/10.3390/ijms22137141.

Gottschalk, F., Nowack, B., 2011. The release of engineered nanomaterials to the environment. J. Environ. Monit. 13, 1145–1155. https://doi.org/10.1039/C0EM00547A.

Graça, M.A.S., 2001. The role of invertebrates on leaf litter decomposition in streams – a review. Int. Rev. Hydrobiol. 86, 383–393. https://doi.org/10.1002/1522-2632(200107)86:4/5%3C383::AID-IROH383%3E3.0.CO;2-D.

Graça, M.A.S., Canhoto, C., 2006. Leaf litter processing in low order streams. Limnética 25, 1–10. https://doi.org/10.23818/limn.25.01.
Hartmann, N.B., Hüffer, T., Thompson, R.C., Hassellöv, M., Verschoor, A., Daugaard, A. E., Rist, S., Karlsson, T., Brennholt, N., Cole, M., Herrling, M.P., Hess, M.C., Ivleva, N. P., Lusher, A.L., Wagner, M., 2019. Are we speaking the same language? Recommendations for a definition and categorization framework for plastic debris. Environ. Sci. Technol. 53, 1039–1047. https://doi.org/10.1021/acs.est.8b05297.
Jambeck, J., Roland, G., Chris, W., Siegler, T.R., Miriam, P., Anthony, A., Ramani, N., Lavender, L.K., 2015. Plastic waste inputs from land into the ocean. Science 347, 768–771. https://doi.org/10.1126/science.1260352, 1979.
Keller, A.A., Adeleye, A.S., Conway, J.R., Garner, K.L., Zhao, L., Cherr, G.N., Hong, J., Gardea-Torresdey, J.L., Godwin, H.A., Hanna, S., Ji, Z., Kaweeteerawat, C., Lin, S., Lenihan, H.S., Miller, R.J., Nel, A.E., Peralta-Videa, J.R., Walker, S.L., Taylor, A.A., Torres-Duarte, C., Zink, J.I., Zuverza-Mena, N., 2017. Comparative environmental fate and toxicity of copper nanomaterials. Nano Impact 7, 28–40. https://doi.org/10.1016/j.impact.2017.05.003.
Kik, K., Bukowska, B., Sicińska, P., 2020. Polystyrene nanoparticles: sources, occurrence in the environment, distribution in tissues, accumulation and toxicity to various organisms. Environ. Pollut. 262, 114297 https://doi.org/10.1016/j.envpol.2020.114297.
Koelmans, A.A., Besseling, E., Wegner, A., Foekema, E.M., 2013. Plastic as a carrier of POPs to aquatic organisms: a model analysis. Environ. Sci. Technol. 47, 7812–7820. https://doi.org/10.1021/es401169n.
Krauss, G.-J., Solé, M., Krauss, G., Schlosser, D., Wesenberg, D., Bärlocher, F., 2011. Fungi in freshwaters: ecology, physiology and biochemical potential. FEMS Microbiol. Rev. 35, 620–651. https://doi.org/10.1111/j.1574-6976.2011.00266.x.
Kumar, M., Chen, H., Sarsaiya, S., Qin, S., Liu, H., Awasthi, M.K., Kumar, S., Singh, L., Zhang, Z., Bolan, N.S., Pandey, A., Varjani, S., Taherzadeh, M.J., 2021. Current research trends on micro- and nano-plastics as an emerging threat to global environment: a review. J. Hazard Mater. 409, 124967 https://doi.org/10.1016/j.jhazmat.2020.124967.
Kumar, S., Koh, J., 2014. Physiochemical and optical properties of chitosan-based graphene oxide bionanocomposite. Int. J. Biol. Macromol. 70, 559–564. https://doi.org/10.1016/j.ijbiomac.2014.07.019.
Kumar, S., Kumar Mishra, D., Sobral, A.J.F.N., Koh, J., 2019. CO_2 adsorption and conversion of epoxides catalyzed by inexpensive and active mesoporous structured mixed-phase (anatase/brookite) TiO_2. J. CO2 Util. 34, 386–394. https://doi.org/10.1016/j.jcou.2019.07.019.
Lee, W.S., Cho, H.-J., Kim, E., Huh, Y.H., Kim, H.-J., Kim, B., Kang, T., Lee, J.-S., Jeong, J., 2019. Bioaccumulation of polystyrene nanoplastics and their effect on the toxicity of Au ions in zebrafish embryos. Nanoscale 11, 3173–3185. https://doi.org/10.1039/C8NR09321K.
Lenz, R., Enders, K., Torkel-Gissel, N., 2016. Microplastic exposure studies should be environmentally realistic. Proc. Natl. Acad. Sci. USA 113, E4121–E4122. https://doi.org/10.1073/pnas.1606615113.
Li, P., Li, Q., Hao, Z., Yu, S., Liu, J., 2020. Analytical methods and environmental processes of nanoplastics. J. Environ. Sci. 94, 88–99. https://doi.org/10.1016/j.jes.2020.03.057.
Liu, J., Ma, Y., Zhu, D., Xia, T., Qi, Y., Yao, Y., Guo, X., Ji, R., Chen, W., 2018. Polystyrene nanoplastics-enhanced contaminant transport: role of irreversible adsorption in glassy polymeric domain. Environ. Sci. Technol. 52, 2677–2685. https://doi.org/10.1021/acs.est.7b05211.
Loos, C., Syrovets, T., Musyanovych, A., Mailänder, V., Landfester, K., Nienhaus, G.U., Simmet, T., 2014. Functionalized polystyrene nanoparticles as a platform for studying bio-nano interactions. Beilstein J. Nanotechnol. 5, 2403–2412. https://doi.org/10.3762/bjnano.5.250.
Mattsson, K., Jocic, S., Doverbratt, I., Hansson, L.-A., 2018. In: Zeng, E.Y. (Ed.), Microplastic Contamination in Aquatic Environments. Chapter 13 – Nanoplastics in the Aquatic Environment. Elsevier, pp. 379–399. https://doi.org/10.1016/B978-0-12-813747-5.00013-8.
Miao, L., Hou, J., You, G., Liu, Z., Liu, S., Li, T., Mo, Y., Guo, S., Qu, H., 2019. Acute effects of nanoplastics and microplastics on periphytic biofilms depending on particle size, concentration and surface modification. Environ. Pollut. 255, 113300 https://doi.org/10.1016/j.envpol.2019.113300.
Miersch, J., Bärlocher, F., Bruns, I., 1997. Effects of cadmium, copper, and zinc on growth and thiol content of aquatic hyphomycetes. Hydrobiologia 346, 77–84. https://doi.org/10.1023/A:1002957830704.
Minelli, C., Bartczak, D., Peters, R., Rissler, J., Undas, A., Sikora, A., Sjöström, E., Goenaga-Infante, H., Shard, A.G., 2019. Sticky measurement problem: number concentration of agglomerated nanoparticles. Langmuir 35, 4927–4935. https://doi.org/10.1021/acs.langmuir.8b04209.
Mueller, N.C., Nowack, B., 2008. Exposure modeling of engineered nanoparticles in the environment. Environ. Sci. Technol. 42, 4447–4453. https://doi.org/10.1021/es7029637.
Munier, B., Bendell, L.I., 2018. Macro and micro plastics sorb and desorb metals and act as a point source of trace metals to coastal ecosystems. PLoS One 13, e0191759. https://doi.org/10.1371/journal.pone.0191759.
Naqash, N., Prakash, S., Kapoor, D., Singh, R., 2020. Interaction of freshwater microplastics with biota and heavy metals: a review. Environ. Chem. Lett. 18, 1813–1824. https://doi.org/10.1007/s10311-020-01044-3.
Nath, J., Dror, I., Berkowitz, B., 2020. Effect of nanoplastics on the transport of platinum-based pharmaceuticals in water-saturated natural soil and their effect on a soil microbial community. Environ. Sci.: Nano 7, 3178–3188. https://doi.org/10.1039/D0EN00651C.
Nolte, T.M., Hartmann, N.B., Kleijn, J.M., Garnæs, J., van de Meent, D., Jan Hendriks, A., Baun, A., 2017. The toxicity of plastic nanoparticles to green algae as influenced by surface modification, medium hardness and cellular adsorption. Aquat. Toxicol. 183, 11–20. https://doi.org/10.1016/j.aquatox.2016.12.005.
Nowack, B., Ranville, J.F., Diamond, S., Gallego-Urrea, J.A., Metcalfe, C., Rose, J., Horne, N., Koelmans, A.A., Klaine, S.J., 2012. Potential scenarios for nanomaterial release and subsequent alteration in the environment. Environ. Toxicol. Chem. 31, 50–59. https://doi.org/10.1002/etc.726.
Petersen, E.J., Nelson, B.C., 2010. Mechanisms and measurements of nanomaterial-induced oxidative damage to DNA. Anal. Bioanal. Chem. 398, 613–650. https://doi.org/10.1007/s00216-010-3881-7.
Pikuda, O., Xu, E.G., Berk, D., Tufenkji, N., 2019. Toxicity assessments of micro- and nanoplastics can Be confounded by preservatives in commercial formulations. Environ. Sci. Technol. Lett. 6, 21–25. https://doi.org/10.1021/acs.estlett.8b00614.
Pradhan, A., Seena, S., Schlosser, D., Gerth, K., Helm, S., Dobritzsch, M., Krauss, G.-J., Dobritzsch, D., Pascoal, C., Cássio, F., 2015. Fungi from metal-polluted streams may have high ability to cope with the oxidative stress induced by copper oxide nanoparticles. Environ. Toxicol. Chem. 34, 923–930. https://doi.org/10.1002/etc.2879.
Pradhan, A., Seena, S., Dobritzsch, D., Helm, S., Gerth, K., Dobritzsch, M., Krauss, G.-J., Schlosser, D., Pascoal, C., Cássio, F., 2014. Physiological responses to nano CuO in fungi from non-polluted and metal-polluted streams. Sci. Total Environ. 466, 556–563. https://doi.org/10.1016/j.scitotenv.2013.07.073, 467.
Prasad, R., Bhattacharyya, A., Nguyen, Q.D., 2017. Nanotechnology in sustainable agriculture: recent developments, challenges, and perspectives. Front. Microbiol. 8 https://doi.org/10.3389/fmicb.2017.01014.
Qu, M., Miao, L., Chen, H., Zhang, X., Wang, Y., 2023. SKN-1/Nrf2-dependent regulation of mitochondrial homeostasis modulates transgenerational toxicity induced by nanoplastics with different surface charges in Caenorhabditis elegans. J. Hazard Mater. 457, 131840 https://doi.org/10.1016/j.jhazmat.2023.131840.
Quainoo, S., Seena, S., Graça, M.A.S., 2016. Copper tolerant ecotypes of Heliscus lugdunensis differ in their ecological function and growth. Sci. Total Environ. 544, 168–174. https://doi.org/10.1016/j.scitotenv.2015.11.119.
Qv, W., Wang, X., Li, N., Du, J., Pu, G., Zhang, H., 2022. How do the growth and metabolic activity of aquatic fungi Geotrichum candidum and Aspergillus Niger respond to nanoplastics? Bull. Environ. Contam. Toxicol. 109, 1043–1050. https://doi.org/10.1007/s00128-022-03625-0.
Salata, O.V., 2004. Applications of nanoparticles in biology and medicine. J. Nanobiotechnol. 2, 3. https://doi.org/10.1186/1477-3155-2-3.
Santos, D., Luzio, A., Matos, C., Bellas, J., Monteiro, S.M., Félix, L., 2021. Microplastics alone or co-exposed with copper induce neurotoxicity and behavioral alterations on zebrafish larvae after a subchronic exposure. Aquat. Toxicol. 235, 105814 https://doi.org/10.1016/j.aquatox.2021.105814.
Schneider, C.A., Rasband, W.S., Eliceiri, K.W., 2012. NIH Image to ImageJ: 25 years of image analysis. Nat. Methods 9, 671–675. https://doi.org/10.1038/nmeth.2089.
Seena, S., Gutiérrez, I.B., Barros, J., Nunes, C., Marques, J.C., Kumar, S., Gonçalves, A.M. M., 2022a. Impacts of low concentrations of nanoplastics on leaf litter decomposition and food quality for detritivores in streams. J. Hazard Mater. 429, 128320 https://doi.org/10.1016/j.jhazmat.2022.128320.
Seena, S., Baschien, C., Barros, J., Sridhar, K.R., Graça, M.A.S., Mykrä, H., Bundschuh, M., 2022b. Ecosystem services provided by fungi in freshwaters: a wake-up call. Hydrobiologia. https://doi.org/10.1007/s10750-022-05030-4.
Seena, S., Duarte, S., Pascoal, C., Cássio, F., 2012. Intraspecific variation of the aquatic fungus Articulospora tetracladia: an ubiquitous perspective. PLoS One 7, e35884. https://doi.org/10.1371/journal.pone.0035884.
Seena, S., Graça, D., Bartels, A., Cornut, J., 2019. Does nanosized plastic affect aquatic fungal litter decomposition? Fungal Ecol 39, 388–392. https://doi.org/10.1016/j.funeco.2019.02.011.
Seena, S., Kumar, S., 2019. Short-term exposure to low concentrations of copper oxide nanoparticles can negatively impact the ecological performance of a cosmopolitan freshwater fungus. Environ Sci Process Impacts 21, 2001–2007. https://doi.org/10.1039/C9EM00361D.
Seena, S., Marvanová, L., Letourneau, A., Bärlocher, F., 2018. *Articulospora* – phylogeny vs morphology. Fungal Biol. 122, 965–976. https://doi.org/10.1016/j.funbio.2018.06.001.
Seena, S., Sobral, O., Cano, A., 2020. Metabolomic, functional, and ecologic responses of the common freshwater fungus *Neonectria lugdunensis* to mine drainage stress. Sci. Total Environ. 718, 137359 https://doi.org/10.1016/j.scitotenv.2020.137359.
Solé, M., Fetzer, I., Wennrich, R., Sridhar, K.R., Harms, H., Krauss, G., 2008. Aquatic hyphomycete communities as potential bioindicators for assessing anthropogenic stress. Sci. Total Environ. 389, 557–565. https://doi.org/10.1016/j.scitotenv.2007.09.010.
Solé, M., Müller, I., Pecyna, M.J., Fetzer, I., Harms, H., Schlosser, D., 2012. Differential regulation by organic compounds and heavy metals of multiple laccase genes in the aquatic hyphomycete *Clavariopsis aquatica*. Appl. Environ. Microbiol. 78, 4732–4739. https://doi.org/10.1128/AEM.00635-12.
Sridhar, K.R., Krauss, G., Bärlocher, F., Wennrich, R., Krauss, G.J., 2000. Fungal diversity in heavy metal polluted waters in central Germany. Fungal Divers. 5, e129.
Tallec, K., Blard, O., González-Fernández, C., Brotons, G., Berchel, M., Soudant, P., Huvet, A., Paul-Pont, I., 2019. Surface functionalization determines behavior of nanoplastic solutions in model aquatic environments. Chemosphere 225, 639–646. https://doi.org/10.1016/j.chemosphere.2019.03.077.
Thompson, R.C., Moore, C.J., vom Saal, F.S., Swan, S.H., 2009. Plastics, the environment and human health: current consensus and future trends. Philos. Trans. R. Soc. Lond. B Biol. Sci. 364, 2153–2166. https://doi.org/10.1098/rstb.2009.0053.
Wagner, M., Scherer, C., Alvarez-Muñoz, D., Brennholt, N., Bourrain, X., Buchinger, S., Fries, E., Grosbois, C., Klasmeier, J., Marti, T., Rodriguez-Mozaz, S., Urbatzka, R., Vethaak, A.D., Winther-Nielsen, M., Reifferscheid, G., 2014. Microplastics in

freshwater ecosystems: what we know and what we need to know. Environ. Sci. Eur. 26, 12. https://doi.org/10.1186/s12302-014-0012-7.

Wan, J.-K., Chu, W.-L., Kok, Y.-Y., Lee, C.-S., 2021. Influence of polystyrene microplastic and nanoplastic on copper toxicity in two freshwater microalgae. Environ. Sci. Pollut. Res. 28, 33649–33668. https://doi.org/10.1007/s11356-021-12983-x.

Wang, L., Wu, W.-M., Bolan, N.S., Tsang, D.C.W., Li, Y., Qin, M., Hou, D., 2021. Environmental fate, toxicity and risk management strategies of nanoplastics in the environment: current status and future perspectives. J. Hazard Mater. 401, 123415 https://doi.org/10.1016/j.jhazmat.2020.123415.

Xu, D., Ma, Y., Han, X., Chen, Y., 2021. Systematic toxicity evaluation of polystyrene nanoplastics on mice and molecular mechanism investigation about their internalization into Caco-2 cells. J. Hazard Mater. 417, 126092 https://doi.org/10.1016/j.jhazmat.2021.126092.

Yang, M., Wang, W.-X., 2023. Recognition and movement of polystyrene nanoplastics in fish cells. Environ. Pollut. 316, 120627 https://doi.org/10.1016/j.envpol.2022.120627.

Zhang, F., Li, D., Yang, Y., Zhang, H., Zhu, J., Liu, J., Bu, X., Li, E., Qin, J., Yu, N., Chen, L., Wang, X., 2022a. Combined effects of polystyrene microplastics and copper on antioxidant capacity, immune response and intestinal microbiota of Nile tilapia (*Oreochromis niloticus*). Sci. Total Environ. 808, 152099 https://doi.org/10.1016/j.scitotenv.2021.152099.

Zhang, F., Wang, Z., Wang, S., Fang, H., Wang, D., 2019. Aquatic behavior and toxicity of polystyrene nanoplastic particles with different functional groups: complex roles of pH, dissolved organic carbon and divalent cations. Chemosphere 228, 195–203. https://doi.org/10.1016/j.chemosphere.2019.04.115.

Zhang, H., Cheng, H., Wang, Y., Duan, Z., Cui, W., Shi, Y., Qin, L., 2022b. Influence of functional group modification on the toxicity of nanoplastics. Front. Mar. Sci. 8 https://doi.org/10.3389/fmars.2021.800782.

Zhang, Y., Cheng, F., Zhang, T., Li, C., Qu, J., Chen, J., Peijnenburg, W.J.G.M., 2022c. Dissolved organic matter enhanced the aggregation and oxidation of nanoplastics under simulated sunlight irradiation in water. Environ. Sci. Technol. 56, 3085–3095. https://doi.org/10.1021/acs.est.1c07129.